Sensors and Materials, Vol. 21, No. 5 (2009) 259–264
MYU Tokyo

S & M 0766

WO_3 Crystals and Their NO_2-Sensing Properties

Zhicong Meng*, Chizumi Kitagawa,
Akari Takahashi, Yu Okochi and Jun Tamaki

Department of Applied Chemistry, College of Life Science,
Ritsumeikan University, Kusatsu-shi, Shiga 525-8577, Japan

(Received April 6, 2009; accepted June 1, 2009)

Key words: WO_3 sensor, semiconductor sensor, gas sensor, NO_2 detection

WO_3 film sensors with various crystalline morphologies have been investigated for highly sensitive detection of dilute NO_2. Four types of WO_3 particles, spherical, disk, cuboid, and hexagonal, were prepared by pyrolysis (spherical), precipitation method (disk), and hydrothermal synthesis under different conditions (cuboid and hexagonal). WO_3 film sensors were fabricated on Au comb-type microelectrodes by suspension dropping using the various WO_3 powders obtained, and their sensor properties to dilute NO_2 were investigated at 200°C. The cuboid WO_3 film sensor showed the best response-recovery property with 90% response and 90% recovery times of 1.3 and 0.9 min to 0.05 ppm NO_2 at 200°C, respectively. The hexagonal WO_3 film sensor showed extremely high sensitivity of 41.1 to 0.01 ppm NO_2 at 200°C. The sensor performance suggested the possibility of environmental monitoring of dilute NO_2 using WO_3 film sensors.

1. Introduction

It is well known that the detection and emission control of nitrogen oxides (NO_x: NO and NO_2) are crucial points to reduce the noxious effects of occurences, such as acid rain, photochemical smog, and production of ozone on the environment and human beings. Semiconductor gas sensors based on metal oxides have been studied extensively,[1,2] and WO_3 has been demonstrated to be an excellent sensing material for NO_x detection.[3–5] It was found that the sensitivity to dilute NO_2 can be much improved using a thin film structure,[6–8] and WO_3-based thin-film sensors are able to detect dilute NO_2 below the ppm level. In previous publications,[9,10] we reported on the thickness effect of WO_3 thin-film sensors, the performance of WO_3 thick-film sensors and their sensing mechanisms. In this study, WO_3 film sensors, were constructed using four types of WO_3 particles with various crystalline morphologies, and their sensing properties in dilute NO_2 detection were investigated.

*Corresponding author: e-mail: mou@fc.ritsumei.ac.jp

2. Experiments

WO_3 particles exhibit various crystalline morphologies depending on their preparation process. In this work, spherical, disk, cuboid, and hexagonal WO_3 particles were prepared and used to fabricate sensor elements. The sensing properties of the various WO_3 film sensors to dilute NO_2 have been investigated.

Spherical WO_3 particles were prepared by pyrolysis of $(NH_4)_{10}W_{12}O_{41}\cdot 5H_2O$ in air at 850°C for 4 h. Disk WO_3 particles were prepared by the precipitation method. An aqueous solution of $(NH_4)_{10}W_{12}O_{41}\cdot 5H_2O$ was neutralized with nitric acid, and the precipitate (H_2WO_4) obtained was filtrated, washed, and calcined at 400°C for 3 h in air. Cuboid WO_3 particles were prepared by hydrothermal synthesis. The H_2WO_4 precipitate obtained by precipitation, which is the same as that in the preparation of disk WO_3 particles, was placed in a pressure-resistant airtight container with ion-exchanged water, and underwent hydrothermal synthesis at 160°C for 14 h. Hexagonal WO_3 particles were also prepared by hydrothermal synthesis, but unlike in the preparation of cuboid WO_3 particles, the H_2WO_4 precipitate was hydrothermally synthesized with ion-exchanged water and a surfactant, cetyltrimethylammonium bromide (CTAB), at 150°C for 10 h. The product was found to be a mixture of cuboid and hexagonal WO_3 particles. However, a preparation method for pure hexagonal WO_3 particles has not yet been discovered.

The crystal structure and grain size of the various WO_3 particles obtained were evaluated by X-ray diffraction (XRD: Rigaku, Rint-2200) and field-emission scanning electron microscopy (FE-SEM: Hitachi, S-4800), and the results are shown in Figs. 1 and

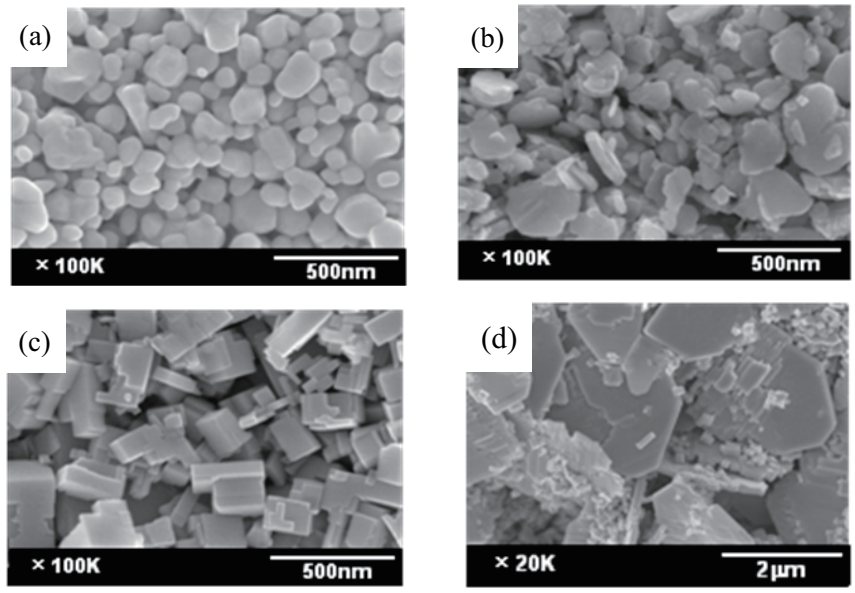

Fig. 1. SEM images of various WO_3 particles: (a) spherical WO_3, (b) disk WO_3, (c) cuboid WO_3, and (d) hexagonal WO_3.

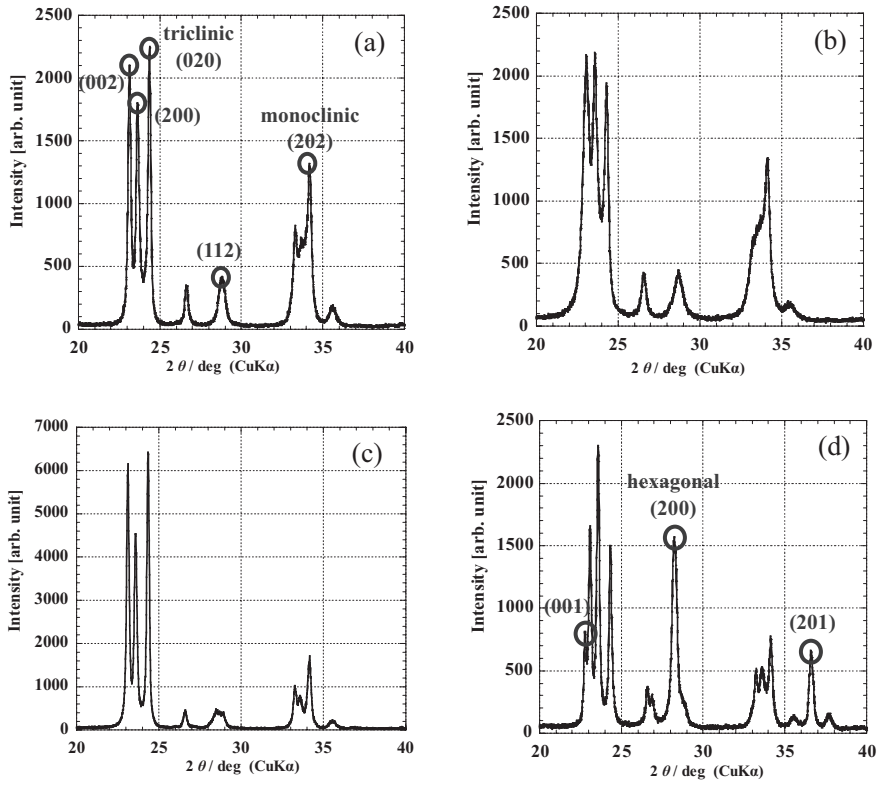

Fig. 2. XRD pattern of various WO_3 particles: (a) spherical WO_3, (b) disk WO_3, (c) cuboid WO_3, and (d) hexagonal WO_3.

2, respectively. The grains sizes of the spherical WO_3 particles were estimated to be 70 –150 nm in diameter. Disk WO_3 particles were estimated to be 50–200 nm in diameter with a thickness of 20–30 nm. Cuboid WO_3 particles were rectangular-shaped with a side length of 50–200 nm, and hexagonal WO_3 particles were hexagonal-disc-shaped with a side length of 0.7–1 μm with a thickness of 20–30 nm. From XRD analysis, the crystal structures of the spherical, disk, and cuboid WO_3 powders were confirmed to be triclinic mixed with a monoclinic crystal system, and the hexagonal WO_3 was crystallized in a hexagonal system.

WO_3 films were fabricated by suspension dropping on a SiO_2/Si substrate equipped with Au comb-type microelectrodes (line width: 2 μm, distance between lines: 2 μm, and electrode area: 0.5 × 0.5 mm^2, without backside heater). A small amount of suspension, which was obtained by mixing WO_3 powder with ion-exchanged water, was dropped onto the Au comb-type microelectrodes, dried, and calcined in air at 400°C for 3 h. Figure 3 shows a schematic drawing of the sensor element. The film thickness could be controlled in the range of 10–15 μm by changing the WO_3 powder concentration in

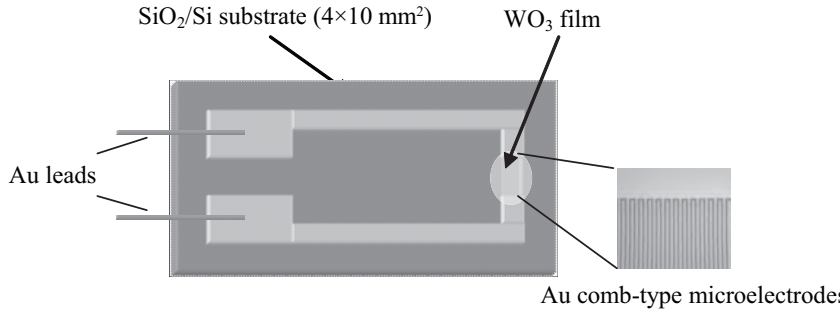

Fig. 3. Schematic drawing of WO_3 film NO_2 sensor.

suspension and the dropping amount of suspension. The surface morphology of the films was confirmed by FE-SEM, which showed that the comb-type-microelectrode area was completely covered by WO_3 grains.

In the measurement of NO_2-sensing properties, the WO_3 film sensors were set into a flow apparatus. The electrical resistances of the sensor elements were measured in dry air (R_a) and in NO_2-containing dry air (R_g) at 200°C. The sensitivity (S) was defined as the ratio of R_g to R_a ($S = R_g/R_a$). The NO_2 concentration was varied in the range of 0.01–0.5 ppm. A 5.37 ppm NO_2 (N_2 balance) tank and a pure O_2 tank were employed to prepare the dilute NO_2 in the above concentration range, and the flow rate was maintained at 100 ml/min.

3. Results and Discussion

Figure 4 shows the sensitivities to dilute NO_2 of four WO_3 film sensors at 200°C as a function of NO_2 concentration, and Fig. 5 shows the response transient of the various sensor elements to 0.05 ppm NO_2 at 200°C. The sensing properties to dilute NO_2 of various WO_3 film sensors are summarized in Table 1. The sensitivity of the spherical WO_3 film sensor to dilute NO_2 was the lowest among the four sensors. It was predicted that, owing to the low-density packing of spherical-shaped WO_3 particles, diffusion of oxygen into the WO_3 film occurs easily, while adsorption of NO_2 is suppressed, and thus there is a decrease in sensitivity to NO_2.[10] The sensitivities of the disk and cuboid WO_3 film sensors were similar. To 0.01 ppm NO_2, the sensitivity was 6–10, while the response-recovery characteristics showed that the cuboid WO_3 film sensor has the best recovery property among the four sensors. The 90% response and 90% recovery times were 1.3 and 0.9 min to 0.05 ppm NO_2 at 200°C, respectively. During the experiments, the response-recovery characteristics of the sensor were almost unchanged to 0.01–0.5 ppm NO_2. In the four sensors, the hexagonal WO_3 sensor showed the highest sensitivity to dilute NO_2. The sensitivity to 0.01 ppm NO_2 at 200°C was as high as 41.1. Although the response-recovery of the hexagonal WO_3 sensor was somewhat slower than those of the other three sensors, the extremely high sensitivity to low-concentration NO_2 is the most attractive feature in applications for highly dilute NO_2 detection. It is presumed

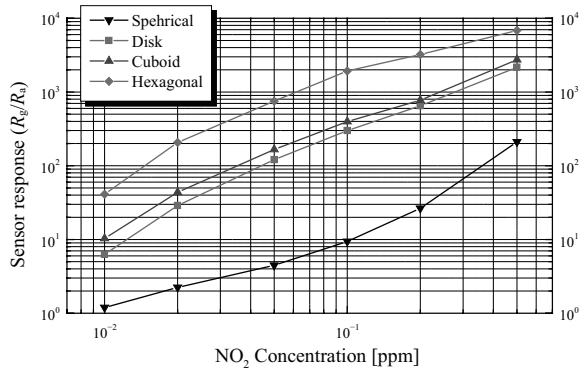

Fig. 4. Sensitivities to NO_2 of WO_3 film sensors as a function of NO_2 concentration (operating temperature: 200°C).

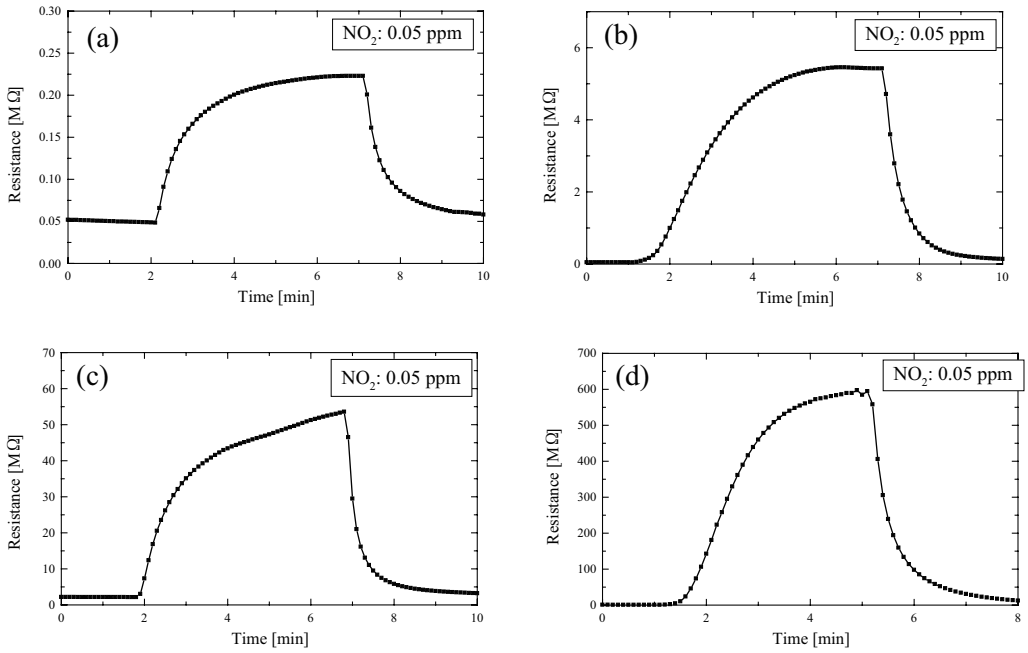

Fig. 5. Response transients of various WO_3 film sensors to 0.05 ppm NO_2 at 200°C: (a) spherical WO_3, (b) disk WO_3, (c) cuboid WO_3, and (d) hexagonal WO_3.

that the extremely high sensitivity of the hexagonal WO_3 film sensor may be due to the much higher adsorptivity of the film structure formed by the hexagonal WO_3 particles, or an extremely high NO_2 adsorption face within the hexagonal WO_3 particles. Further studies on the sensing mechanism are in progress.

Table 1
NO_2-sensing properties of various WO_3 film sensors (operating temperature: 200°C)

WO_3 particle	Film thickness (μm)	T_{90} of response (min)	T_{90} of recovery (min)	$S_{0.01\ ppm\ NO_2}$ (R_g/R_a)
Spherical	10.6	2.1	1.4	1.2
Disk	17.8	2.0	1.1	6.3
Cuboid	11.5	1.3	0.9	10.3
Hexagonal	14.4	2.4	1.4	41.1

4. Conclusions

Four types of WO_3 particles, spherical, disk, cuboid, and hexagonal, were prepared by pyrolysis, precipitation method, and hydrothermal synthesis under various conditions, respectively. WO_3 film sensors are fabricated on Au comb-type microelectrodes by suspension dropping using the various WO_3 powders obtained, and their sensor properties to dilute NO_2 from 0.01 to 0.5 ppm were investigated at 200°C. The cuboid WO_3 film sensor shows the best response-recovery property with 90% response and 90% recovery times of 1.3 and 0.9 min to 0.05 ppm NO_2 at 200°C, respectively. The hexagonal WO_3 film sensor shows an extremely high sensitivity of 41.1 to 0.01 ppm NO_2 at 200°C. The sensor performance suggests possibilities for environmental monitoring and applications requiring highly dilute NO_2 detection.

Acknowledgment

This research was partially supported by the Japanese Ministry of Environment under the project of "Promotion for Environmental Technology." The subject of the research is "Development of a compact and high-sensitivity semiconductor NO_2 gas sensor setting at road neighbor for environmental measurements."

References

1 G. Faglia, G. Benussi, L. Depero, G. Dinelli and G. Sberveglieri: Sens. Mater. **8** (1996) 239.
2 T. Inoue, K. Ohtsuka, Y. Yoshida, Y. Matsuura and Y. Kajiyama: Sens. Actuators, B **24,25** (1995) 388.
3 M. Akiyama, J. Tamaki, N. Miura and N. Yamazoe: Chem. Lett. **20** (1991) 1611.
4 G. Sberveglieri, L. Depero, S. Groppelli and P. Nelli: Sens. Actuators, B **26,27** (1995) 89.
5 J. Tamaki, Z. Zhang, K. Fujimori, M. Akiyama, T. Harada, N. Miura and N. Yamazoe: J. Electrochem. Soc. **141** (1994) 2207.
6 C. Cantalini, M. Pelino, H. T. Sun, M. Faccio, S. Santucci, L. Lozzi and M. Passacantando: Sens. Actuators, B **35,36** (1996) 112.
7 C. Cantalini, W. Wlodarski , Y. Li, M. Passacantando, S. Santucci, E. Comini, G. Faglia and G. Sberveglieri: Sens. Actuators, B **64** (2000) 182.
8 T.-S. Kim, Y.-B. Kim, K.-S. Yoo, G.-S. Sung and H.-J. Jung: Sens. Actuators, B **62** (2000) 102.
9 J. Tamaki, A. Hayashi, Y. Yamamoto and M. Matsuoka: Sens. Actuators, B **95** (2003) 111.
10 J. Tamaki, A. Hayashi and Y. Yamamoto: J. Ceram. Soc. Jpn. PacRim5 Special Issue **112** (2004) S546.